Biochem. J. (1996) **315**, 715–720 (Printed in Great Britain)

RESEARCH COMMUNICATION

Structures of diphospho-*myo*-inositol pentakisphosphate and bisdiphospho-*myo*-inositol tetrakisphosphate from *Dictyostelium* resolved by NMR analysis

Tim LAUSSMANN, Reint EUJEN, C. Michael WEISSHUHN, Ulrich THIEL and Günter VOGEL*

Fachbereich 9 – Chemie, Bergische Universität GHS Wuppertal, Gaußstraße 20, D-42097 Wuppertal, Federal Republic of Germany

Diphospho-*myo*-inositol phosphates (PP-InsP_5 and bis-PP-InsP_4) were isolated from *Dictyostelium* in order to clarify the precise positional isomerism by two-dimensional ^{1}H/^{31}P-NMR analysis. The diphosphorylated inositol phosphates are 4-PP-Ins(1,2,3,5,6)P_5 and 4,5-bis-PP-Ins(1,2,3,6)P_4 or their corresponding enantiomers. The *vicinal* arrangement of the diphospho groups with its steric and electrostatic constraints possibly qualifies bis-PP-InsP_4 as a metabolite with high phosphate-group-transfer potential in phosphotransferase reactions.

INTRODUCTION

The large and steadily growing family of naturally occurring *myo*-inositol phosphates has received intensive study owing to their general and specialized biological activities in cell signalling and homoeostasis. The most abundant inositol phosphate, InsP_6, was thought to be the end point of inositol phosphate anabolism, but recently a novel class of highly phosphorylated inositol phosphates containing energy-rich pyrophosphate groups was discovered in *Dictyostelium discoideum* and the compounds were identified as diphospho-*myo*-inositol pentakisphosphate (PP-InsP_5) and bisdiphospho-*myo*-inositol tetrakisphosphate (bis-PP-InsP_4). They are present at intracellular concentrations in the range 0.05–0.30 mM in this organism and hence are almost as abundant as InsP_6 (about 0.6 mM) [1,2].

The same or similar diphosphorylated compounds have been detected in primitive free-living amoebae [3,4], as well as in a number of mammalian cell types [5–7]; consequently they are ancient and ubiquitous in eukaryotic cells. As demonstrated by radioactive labelling, the intracellular pools of these compounds in mammalian cells are relatively small, but a rapid metabolic turnover is observed which arises by the combined action of ATP-dependent kinases and fluoride-sensitive phosphatases coupling the interconversions of InsP_6, PP-InsP_5 and bis-PP-InsP_4 [5–7]. The physiological significance of this substrate cycle is not known, but it is possibly involved in the regulation of cellular processes by substrate phosphorylation. There are several biological functions of diphospho-*myo*-inositol phosphates discussed in literature. Recent *in vitro* studies using mammalian cell lines showed that PP-InsP_5 acts upon proteins involved in vesicle trafficking. PP-InsP_5 specifically binds to coatomer, a Golgi-vesicle–coat-protein complex, and modulates its K^+-channel activity [8]. Additionally, clathrin assembly is blocked by binding of PP-InsP_5 to synapse-specific clathrin-assembly protein (AP3) from bovine brain [9].

A preliminary structural characterization based on ^{31}P-NMR analysis and fast-atom-bombardment MS led to the suggestion that the likeliest structures of the diphospho-*myo*-inositol phosphates isolated from *Dictyostelium* were 1-PP-InsP_5 and 1,4-bis-PP-InsP_4 or their corresponding enantiomers. A *vicinal* arrangement of the two diphospho groups in bis-PP-Ins$P_4$was considered to be unlikely because of steric and electrostatic constraints [1]. Accordingly, the total syntheses of 1-PP-InsP_5 and its enantiomer, 3-PP-InsP_5, were carried out so that their biological functions could be explored. Inhibition studies using non-specific and specific PP-InsP_5 phosphatases led to the suggestion that the enantiomer 1-PP-InsP_5 is the naturally occurring compound [10]. On the other hand, two-dimensional ^{1}H/^{31}P-NMR studies of extracts of the free-living amoebae *Phreatamoeba balamuthi* [3] and *Entamoeba histolytica* [4] indicated that the isomer 5-PP-InsP_5 exists in these species.

In the present study the previously reported isolation procedure for the two diphospho-*myo*-inositol phosphates from *D. discoideum* was optimized and their structures were re-investigated by two-dimensional ^{1}H/^{31}P-NMR analysis in order to elucidate the precise position of the diphospho groups.

MATERIALS AND METHODS

Assay for inositol phosphates

To avoid a time-consuming assay for total phosphorus during anion-exchange chromatography, a simple, semiquantitative complexometric assay for *myo*-inositol phosphates was developed. It is based on the metal-dye-detection method described elsewhere [11,12]. A 1–10 μl portion of the sample, containing 3–100 μM inositol phosphate, were mixed with 1 ml of PAR reagent [10 μM YCl_3 (Aldrich), 70 μM 4-(2-pyridylazo)resorcinol (Fluka), 700 mM Tris/HCl, pH 8.5) and the absorbance was measured at 546 nm. The assay was calibrated using standard solutions of the corresponding inositol phosphate.

Abbreviations used: PP-InsP_5, diphospho-*myo*-inositol pentakisphosphate; bis-PP-InsP_4, bisdiphospho-*myo*-inositol tetrakisphosphate.

* To whom correspondence should be addressed.

Growth of cells and extraction of diphospho-*myo*-inositol phosphates

D. discoideum strain AX2 (A.T.C.C. 24397) was grown in AX2 medium [13] supplemented with 1.8 % maltose instead of glucose at 21 °C in a 10-litre fermenter. Cells were harvested by centrifugation for 10 min at 5000 ***g***, washed with 17 mM phosphate buffer, pH 6.5, and stored at −80 °C. Frozen cells (about 100 g wet weight; 10^{11} cells) were added to 200 ml of 2 M $HClO_4$ containing 50 mM EDTA and mixed vigorously at 0 °C. Denaturated material was removed by centrifugation (10 min, 5000 ***g***). The supernatant was immediately neutralized on ice with 4 M KOH and the precipitate of $KClO_4$ was removed by filtration [11].

Purification of diphospho-*myo*-inositol phosphates

The resulting extract was treated for 15 min with activated charcoal (Norit A; Serva; 2 g/100 ml of extract) to remove nucleotides [11]. After filtration the extract was diluted with distilled water to a final conductivity of 3–4 mS/cm and applied to an 2.5 cm × 20 cm anion-exchange column (Q-Sepharose Fast Flow; Pharmacia). All inositol phosphates, including most of the InsP_6, were eluted with 200 ml of 250 mM HCl. In a second step, the diphospho-*myo*-inositol phosphates containing small amounts of InsP_6 were eluted with 200 ml of 550 mM HCl. The appropriate fractions were combined, immediately neutralized on ice with 4 M LiOH and freeze-dried. The dried samples were desalted by dissolving LiCl in 100 % ethanol (20 ml/g), and the insoluble inositol phosphates were collected from ethanolic suspension by centrifugation (5 min, 6000 ***g***). To separate InsP_6, *PP*-InsP_5 and bis-*PP*-InsP_4, the material obtained from four pre-purified preparations were loaded on a high-resolution 1.6 cm × 10 cm anion-exchange column (Resource Q; Pharmacia) and eluted isocratically with 375 mM HCl. Fractions (1.5 ml each) were collected and analysed by the complexometric assay described above. The fractions containing *PP*-InsP_5 and bis-*PP*-InsP_4 were combined, immediately neutralized on ice with 4 M LiOH and freeze-dried. LiCl was removed with ethanol as described above. The yield and purity of the isolated compounds were examined by the metal-dye-detection HPLC method [11,12] using a high-resolution anion-exchange column (Mono-Q 10/10, Pharmacia).

NMR analysis

The isolated diphospho-*myo*-inositol phosphates were dissolved in 1 ml of ^2H_2O (99.996 % ^2H; Sigma) and freeze-dried. This procedure was repeated twice. The samples were finally dissolved in 0.5 ml of 99.996 % ^2H_2O, the pH was adjusted to 6.0 by titration with [$^2H_4$]acetic acid (99.5 % ^2H; Sigma) and the solutions were filled into 5 mm-diameter NMR tubes.

All spectra were accumulated at 305 K using a Bruker ARX-400 NMR spectrometer equipped with an ASPECT workstation. The resonance frequency was 400.13 MHz for ^1H and 161.98 MHz for ^{31}P.

For one-dimensional ^1H spectra, excitation pulses of 30 ° and relaxation delays of 1.0 s were employed. The spectral width was set to 8474 Hz at a data size of 32768 words, which yields a digital resolution of 0.26 Hz/point. The $^1H^2HO$ signal was suppressed by a selective presaturation pulse. The results are plotted into F_1 of the $^1H/^{31}P$ correlated spectra and in F_1 and F_2 of the $^1H/^1H$ correlated spectra. ^1H chemical shifts are referenced to $^1H^2HO$ (δ 4.70 p.p.m.).

The one-dimensional ^{31}P spectra, plotted into F_2 of the $^1H/^{31}P$ correlated spectra, were obtained with 30 ° excitation pulses and relaxation delays of 0.1 s. The spectral width was 2427 Hz, and, with a data size of 4096 words, the digital resolution was 0.59 Hz/point. For suppression of proton coupling, a WALTZ16 decoupling technique was employed. ^{31}P chemical shifts are referenced to external phosphoric acid.

The ^1H-^1H shift correlated spectra [Figures 1 and 4 (below)] were acquired according to [14] with a selective presaturation pulse of 1.8 s to suppress the $^1H^2HO$ signal at 4.7 p.p.m. Spectral width was 500 Hz in the F_2 (256 points) and 500 Hz in the F^1 domain (128 points), with digital resolutions of 1.95 Hz/point and 3.90 Hz/point respectively. The two-dimensional contour plot resulted, after zero-filling, to a 1024 × 1024 data matrix, applying a sine multiplication without symmetrization.

The two-dimensional $^1H/^{31}P$ correlation spectra (Figures 2 and 3) were recorded with the following pulse sequence [15]: RD–90 ° (^1H)–1/2t_1–180 ° (^{31}P)–1/2t_1–Δ_1–90 ° (^1H) 90 ° (^{31}P)–Δ_2–acquisition. The time intervals Δ_1 and Δ_2 were set to 0.055 s and 0.036 s respectively. Acquired spectra were WALTZ16-proton-decoupled and ^{31}P acquisition time was 0.42 s with 0.5 s recycling delay. Spectral widths were 2439 Hz in the F_2 domain (2048 points) and 1075 Hz in the F_1 domain (128 points), resulting in digital resolutions of 1.2 Hz and 8.4 Hz respectively. The two-dimensional contour plot was obtained after zero-filling to a 2048 × 256 data matrix and applying sine-squared (SSB = 2) multiplication.

RESULTS AND DISCUSSION

The two diphospho-*myo*-inositol phosphates from *Dictyostelium* were separated by high-resolution anion-exchange chromatography of pre-purified $HClO_4$ extracts from *Dictyostelium*. Both isolated compounds were analysed qualitatively and quantitatively using the metal-dye-detection HPLC method [11,12] and were found to be chromatographically pure. Starting from about 4×10^{11} cells, total amounts of 9 μmol of *PP*-InsP_5 and 16 μmol of bis-*PP*-InsP_4 were obtained. This corresponds to yields of 70–80 % with respect to the intracellular concentration of these compounds in vegetative cells [2]. Diphospho-*myo*-inositol phosphates are sensitive to hydrolysis in aqueous solution and therefore should be freeze-dried before storage.

The purified compounds were analysed by ^{31}P- and ^1H-NMR spectroscopy. Best resolution was obtained at pH 6, probably because of favourable intramolecular hydrogen bonding. Several aspects of the structural assignment can be deduced from the one-dimensional NMR spectra.

The ^1H-decoupled ^{31}P-NMR spectra of bis-*PP*-InsP_4 [Figure 2 (below), F_2 domain] show three groups of resonances. Four monophosphate groups are represented by well-resolved singlets between 1.7 and 2.5 p.p.m. The two diphosphates exhibit two groups of upfield resonances. The first group of two doublets near −6 p.p.m. is due to the two β-phosphates, whereas the second pair of doublets around −8.7 p.p.m is further split by $^3J_{P\text{-}H}$ in proton-coupled spectra (not shown) and corresponds to the two α-phosphates. The resonances of each phosphorus in the diphospho groups are split into doublets due to a $^2J_{P\text{-}P}$ coupling ($\approx$17 Hz) between the correlated β- and α-phosphates. Since the corresponding doublets of the two α- and the two β-phosphates exhibit different chemical shifts, a symmetrical arrangement of the diphospho groups to the plane of symmetry (i.e. 1,3 and 4,6) is excluded. Further information is obtained from the ^1H-NMR spectra (Figure 1). Because of the similar magnitude of $^3J_{P\text{-}H}$ and $^3J_{H\text{-}H}$(*trans*) and the fact that $_3J_{H\text{-}H}$(*trans*) is much greater than $^3J_{H\text{-}H}$(*cis*), the signals appear as a doublet (H-2), overlapping triplets (H-1, H-3) and quartets (H-4, H-5, H-6) in medium-resolved spectra. As is general in *myo*-inositol phosphates, the H-

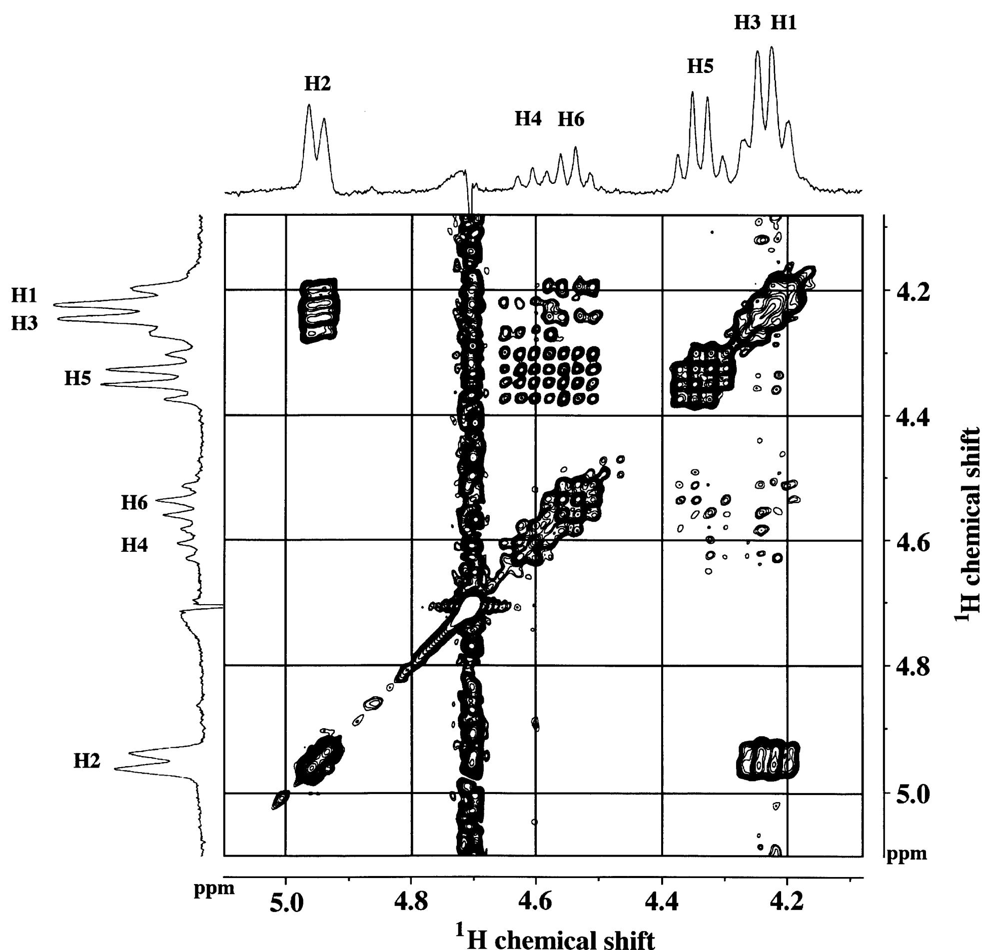

Figure 1 Non-symmetrized two-dimensional ^{1}H–^{1}H shift correlation of Bis-*PP*-InsP_4

2 proton is the only equatorial proton and its resonance is clearly offset (4.94 p.p.m.) from all other proton resonances, showing a characteristic doublet ($^3J_{P\text{-}H}$ 9.9 Hz) of pseudo-triplet pattern with small $^3J_{H\text{-}H}$ couplings of 2.2 Hz to the *cis*-arranged protons H-1 and H-3. Due to diphosphorylation, the spectrum of bis-*PP*-InsP_4 exhibits remarkable differences to the well-documented spectra of InsP_6 [16,17]. The mirror plane of InsP_6 is removed, and a downfield shift of H-4 (4.60 p.p.m.) in comparison with H-6 (4.53 p.p.m.) in bis-*PP*-InsP_4 is observed. The most noticeable difference from the spectrum of InsP_6 is found for the signal of H-5 (4.33 p.p.m.), which is shifted downfield and separated from H-1 and H-3 (4.21 and 4.24 p.p.m. respectively), with respect to the clustered signals of H-1, H-3 and H-5 in the spectrum of InsP_6. This shift of H-5 points to an effect of a diphospho group. To confirm the assignment of the proton resonances, selective decoupling experiments as well as a two-dimensional ^{1}H–^{1}H correlation were performed. Starting from the unambiguously identified H-2 resonance (4.94 p.p.m.), the other signals are readily assigned by the ^{1}H–^{1}H correlation map (Figure 1). Finally, all monophosphates and the diphospho groups were assigned by two-dimensional ^{1}H–^{31}P correlation (Figure 2). The correlation map demonstrates that the α-phosphates of the two diphospho groups are coupled to H-4 and H-5 respectively. Consequently, the diphospho groups in bis-*PP*-InsP_4 are arranged vicinally and the structure is either 4,5-bis-*PP*-D-*myo*-Ins$P$(1,2,3,6)P_4 or its corresponding enantiomer 5,6-bis-*PP*-D-*myo*-Ins(1,2,3,4)P_4. Detailed NMR data are shown in Table 1.

The ^{1}H-decoupled ^{31}P-NMR spectrum of *PP*-InsP_5 (Figure 3, F_2 domain) exhibits five singlets of monophosphates between 1.3 and 2.4 p.p.m. and two doublets ($^2J_{P\text{-}P}$; ≈19 Hz) at −7.23 and −8.70 p.p.m., caused by the β- and the α-phosphate respectively. As in the spectrum of InsP_6, the proton resonance of H-5 (4.26 p.p.m.) is clustered with H-1 and H-3 (4.21 and 4.23 p.p.m. respectively), indicating that position 5 is not diphosphorylated. H-4 (4.58 p.p.m.) remains downfield from H-6 (4.51 p.p.m.), suggesting that position 4 is still diphosphorylated. The assignment of the chemical shifts of the protons was again confirmed by ^{1}H–^{1}H correlation (Figure 4) starting from H-2 (4.94 p.p.m.). The two-dimensional ^{1}H–^{31}P correlation map (Figure 3) finally proves that the diphospho group is bound to position 4. Consequently, the structure of *PP*-InsP_5 is either 4-*PP*-D-*myo*-Ins(1,2,3,5,6)P_5 or its corresponding enantiomer, 6-*PP*-D-*myo*-Ins(1,2,3,4,5)P_5. Detailed NMR data are shown in Table 2.

The unequivocal structural assignment of the two diphospho-*myo*-inositol phosphates was made possible by two-dimensional ^{1}H-^{31}P-NMR correlation. The previous assignments [1] were mainly based on comparison of ^{31}P-NMR spectra of the diphosphorylated compounds with the ^{31}P-NMR spectra of InsP_6. However, the influence of diphosphorylation on the

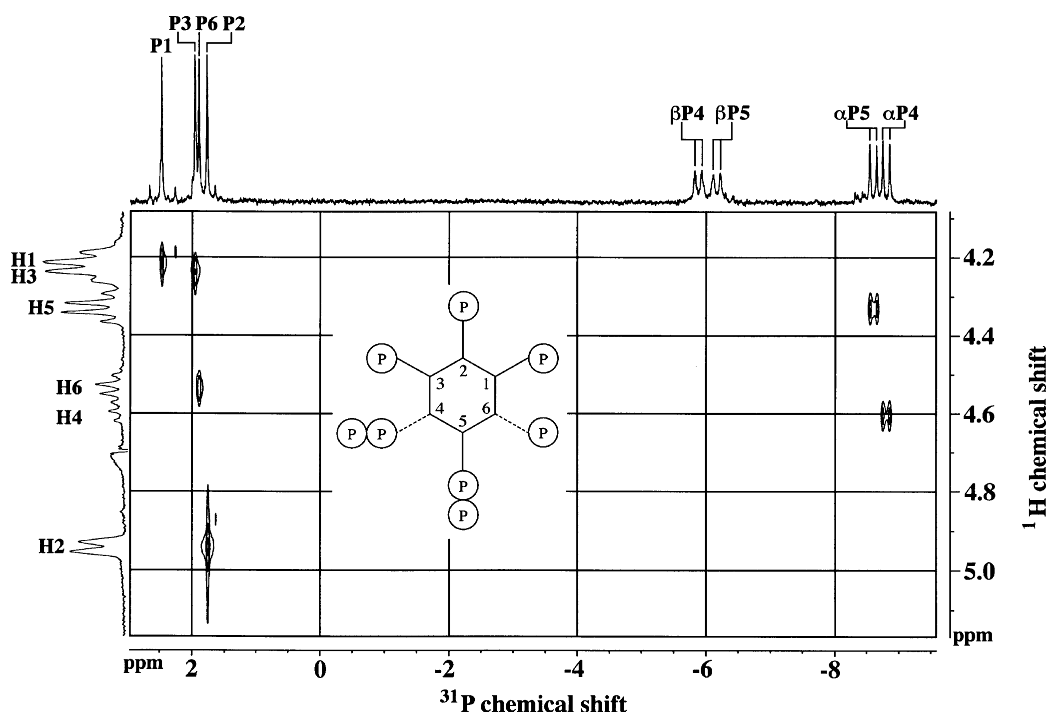

Figure 2 Two-dimensional ^{1}H–^{31}P shift correlation of bis-*PP*-InsP_4

Small resonances observable in the proton-decoupled ^{31}P-NMR spectra plotted into the F_2 domain are due to *PP*-InsP_5, which arises from hydrolytic loss of bis-*PP*-InsP_4 during long-lasting NMR experiments.

Table 1 Detailed NMR data for 4,5-bis-*PP*-Ins(1,2,3,6)P_4

Position	δ P (p.p.m.)	δ H (p.p.m.)	$^{3}J_{P\text{-}H}$ (Hz)	$^{2}J_{P\text{-}P}$ (Hz)
1	2.47	4.21	9.1	–
2	1.76	4.94	9.9	–
3	1.95	4.24	8.7	–
4α	−8.80	4.60	10.0	17.3
4β	−5.88	–	–	17.3
5α	−8.58	4.33	10.0	16.9
5β	−6.17	–	–	16.9
6	1.87	4.53	9.7	–

Table 2 Detailed NMR data for 4-*PP*-Ins(1,2,3,5,6)P_5

Position	δ P (p.p.m.)	δ H (p.p.m.)	$^{3}J_{P\text{-}H}$ (Hz)	$^{2}J_{P\text{-}P}$ (Hz)
1	1.86	4.21	9.0	–
2	1.32	4.94	9.9	–
3	1.77	4.23	9.9	–
4α	−8.70	4.58	9.7	19.1
4β	−7.23	–	–	19.1
5	1.88	4.28	9.9	–
6	2.39	4.51	9.4	–

chemical shifts of the monophosphate groups was not known, and therefore incorrect structures could be deduced from these data.

It is impossible to distinguish between enantiomers by the NMR methods used in the present investigation, but from a biological point of view it seems unlikely that *Dictyostelium* cells produce a mixture of both enantiomers. Nevertheless, some interesting conclusions can be drawn. It is remarkable that the two pyrophosphate groups in 4,5-bis-*PP*-InsP_4 (or 5,6-bis-*PP*-InsP_4) are arranged vicinally. The actual conformation of the compound is not known, but obviously there are high steric constraints and strong electrostatic repulsions due to the highly negative charge density. Therefore the phosphate-group-transfer potential of this compound may be higher than estimated previously [1] and possibly qualifies 4,5-bis-*PP*-InsP_4 as an energy-rich metabolite in hitherto-unknown phosphorylation reactions. Compared with the concentrations in vegetative cells, diphospho-*myo*-inositol phosphates are accumulated in stationary cells and in spores after differentiation (G. Vogel and U. Thiel, unpublished work). From this observation and in line with their high intracellular concentration, it may be speculated that diphospho-*myo*-inositol phosphates are storage molecules and may serve as a unimolecular source of chemical energy, phosphate, carbohydrate and metal ions in ancient organisms like amoebae with a resistant stage in their life cycle. Possibly, different regulatory functions have been evolved in higher eukaryotic cells.

PP-InsP_5 seems to be an intermediate in the synthesis and/or the degradation of bis-*PP*-InsP_4. When isolated from cell extracts, only 4-*PP*-InsP_5 (or its enantiomer 6-*PP*-InsP_5) has been found by NMR analysis. On the other hand, when purified samples of 4,5-bis-*PP*-InsP_4 (or 5,6-bis-*PP*-InsP_4) were partially hydrolysed non-enzymically, both of the possible regioisomers, 5-*PP*-InsP_5 and 4-*PP*-InsP_5 (or 6-*PP*-InsP_5), were observed by NMR analysis (results not shown). Obviously the inositol

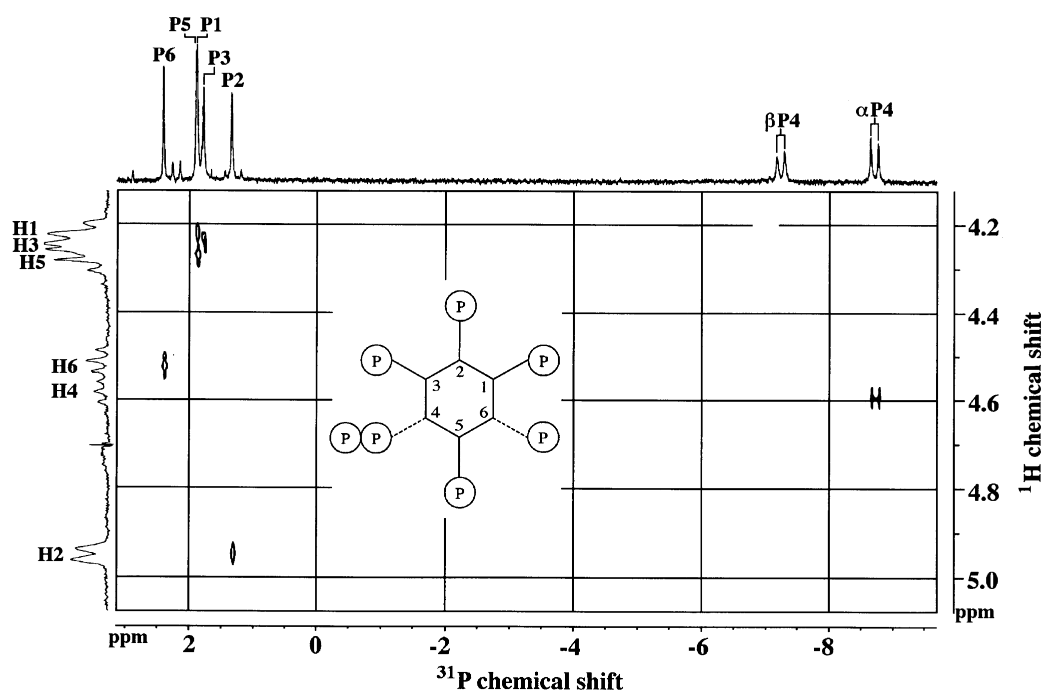

Figure 3 Two-dimensional ^{1}H–^{31}P shift correlation of bis-*PP*-InsP_4

Small resonances observable in the proton-decoupled ^{31}P NMR spectra plotted into the F_2 domain are due to hydrolytic decomposition products, which arise during long-lasting NMR experiments.

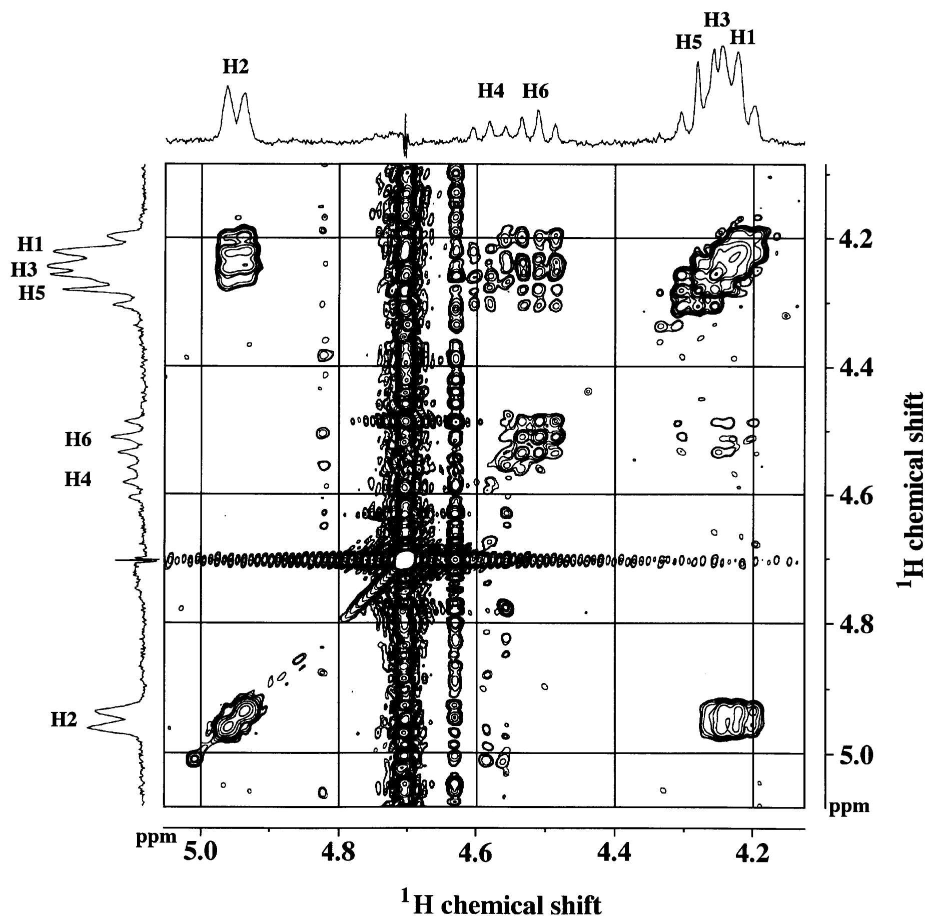

Figure 4 Non-symmetrized two-dimensional ^{1}H–^{1}H shift correlation of *PP*-InsP_4

phosphate metabolism is controlled by a set of rather specific phosphotransferases and phosphatases.

Whether diphospho-*myo*-inositol phosphates observed in different cell types have the same structures as those in *Dictyostelium* is still not known with certainty. Therefore it would be of great interest to analyse them in comparative studies by the metal-dye-detection HPLC method in order to get an uniform view of the inositol phosphate network.

We thank Dr. Hans-Josef Altenbach for providing helpful discussions and Dr. David J. Brauer for critical reading of this manuscript before its submission. We are grateful for the skilled technical assistance of Mrs. Ilka Moeller. This work was supported by the Deutsche Forschungsgemeinschaft (grant VO 348/2-2) and in part by the Fonds der Chemischen Industrie.

REFERENCES

1 Stephens, L., Radenberg, T., Thiel, U., Vogel, G., Khoo, K.-H., Dell, A., Jackson,T. R., Hawkins, P. T. and Mayr, G. W. (1993) J. Biol. Chem. **268**, 4009–4015
2 Mayr, G. W., Radenberg, T., Thiel, U., Vogel, G. and Stephens, L. R. (1992) Carbohydr. Res. **234**, 247–262
3 Martin, J.-B., Bakker-Grunwald, T. and Klein, G. (1995) J. Eukaryotic Microbiol. **42**, 183–191
4 Martin, J.-B., Bakker-Grunwald, T. and Klein, G. (1993) Eur. J. Biochem. **214**, 711–718
5 Menniti, F. S., Miller, R. N., Putney, J. W. and Shears, S. B. (1993) J. Biol. Chem. **268**, 3850–3856
6 Shears, S. B., Ali, N., Craxton, A. and Bembenek, M. E. (1995) J. Biol. Chem. **270**, 10489–10497
7 Glennon, M. C. and Shears, S. B. (1993) Biochem. J. **293**, 583–590
8 Fleischer, B., Xie, J., Mayrleitner, M., Shears, S. B., Palmer, D. J. and Fleischer, S. (1994) J. Biol. Chem. **269**, 17826–17832
9 Ye, W., Ali, N., Bembenek, M. E., Shears, S. B. and Lafer, E. M. (1994) J. Biol. Chem. **270**, 1564–1568
10 Falck, J. R., Reddy, K. K., Ye, J., Saady, M., Mioskowski, C., Shears, S. B., Tan, Z. and Safrany, S. (1995) J. Am. Chem. Soc. **117**, 12172–12175
11 Mayr, G. W. (1990) in Methods in Inositide Research: Mass Determination of Inositol Phosphates by High Performance Liquid Chromatography with Postcolumn Complexometry (Metal Dye Detection) (Irvine, R. F., ed.), pp. 83–108, Raven Press, New York
12 Mayr, G. W. (1988) Biochem. J. **254**, 585–591
13 Watts, D. J. and Asworth, J. M. (1970) Biochem. J. **119**, 171–174
14 Aue, W. P., Bartholdi, E. and Ernst, R. R. (1976) J. Chem. Phys. **64**, 2229–2246
15 Bax, A. and Morris, G. A. (1981) J. Magn. Reson. **42**, 501–505
16 Johnson, K., Barrientos, L. G., Le, L. and Murthy, P. P. N. (1995) Anal. Biochem. **231**, 421–431
17 Scholz, P., Bermann, G. and Mayr, G. W. (1990) in Methods in Inositide Research, Nuclear Magnetic Resonance Spectroscopy of *myo*-Inositol Phosphates (Irvine, R. F., ed.), pp 65–82, Raven Press, New York

Received 13 February 1996/6 March 1996; accepted 7 March 1996